Simulating the Solar System

Sritej Tummuru

Eton College

We first derive Kepler's three Laws and results relating to plotting orbits of planets. We then provide further mathematical and physical analysis of the polar angle versus time graphs for elliptical orbits, and the orbit paths of planets relative to other planets.

1 Variables

a = semi-major axis of ellipse
b = semi-minor axis of ellipse
ϵ = eccentricity of ellipse
G = gravitational constant
M = mass of star
m = mass of planet
θ = angular displacement of planet relative to star

2 Kepler's 3rd Law

By Kepler's 1st law, all planets follow elliptical orbits. The area enclosed by elliptical orbits is:

$$A = \pi ab = \pi a^2\sqrt{1-\epsilon^2} \tag{1}$$

The rate of sweeping out an area is, by Kepler's 2nd Law:

$$\frac{\mathrm{d}A}{\mathrm{d}t} = \frac{1}{2}\sqrt{G(M+m)(1-\epsilon^2)a} \tag{2}$$

which is a constant, as it is independent of t. The time period of the orbit is then:

$$\frac{A}{\frac{\mathrm{d}A}{\mathrm{d}t}} = P = \frac{2\pi a^{\frac{3}{2}}}{\sqrt{G(M+m)}} \tag{3}$$

$$P^2 = \frac{4\pi^2}{G(M+m)}a^3 \tag{4}$$

Which completes the proof. If T is in years and a is in Astronomical Units (AU), then because the Earth must obey the law, and the Earth has $T = 1$ year and $a = 1AU$, the constant of proportionality between T^2 and a^3 must be 1 in this case.

The code in Figure 1 creates a scatter plot of the values of $a^{3/2}$ and T, and then uses linear regression to find the line of best fit of the plotted points. We can see that the gradient of this best fit line is 1 to 5 significant figures.

3 Plotting 2D and 3D Elliptical Orbits

We will prove the polar equation for an ellipse with its leftmost focus at the origin. Recall the Cartesian equation of an ellipse, with semi-major and semi-minor axes a and b respectively, with its centre at the origin:

$$\left(\frac{x}{a}\right)^2 + \left(\frac{y}{b}\right)^2 = 1 \tag{5}$$

Figure 1: A graph that verifies T^2 is proportional to a^3

```
In [6]: semi_major_axes = [0.387, 0.723, 1.000, 1.523, 5.202, 9.576, 19.293, 30.246, 39.509]
        orbital_periods = [0.241, 0.615, 1.000, 1.881, 11.861, 29.628, 84.747, 166.344, 248.348]
        eccentricities = [0.21, 0.01, 0.02, 0.09, 0.05, 0.06, 0.05, 0.01, 0.25]

        semi_major_axes_scaled = [(x ** (3/2)) for x in semi_major_axes]

        fig, ax = plt.subplots()

        ax.scatter(semi_major_axes_scaled, orbital_periods)
        slope, intercept = np.polyfit(semi_major_axes_scaled, orbital_periods, 1)
        ax.plot(np.unique(semi_major_axes_scaled), np.poly1d((slope, intercept))(np.unique(semi_major_axes_scaled)))
        ax.set_xlabel("(a / AU)^(3/2)")
        ax.set_ylabel("T / Yr")
        plt.show()

        print("Gradient of graph (years * AU^(-3/2)): ", slope)
```

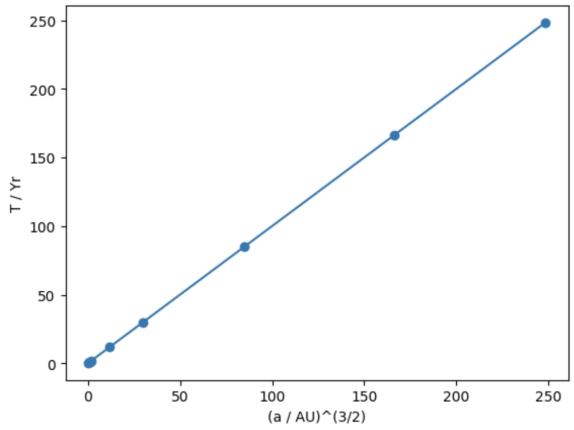


```
Gradient of graph (years * AU^(-3/2)):  1.000036090515211
```

We need a focus to be at the origin, and the distance from the centre to the focus of an ellipse is well known to be $\sqrt{a^2 - b^2}$, so we shift the curve left by $\sqrt{a^2 - b^2}$ to get our final Cartesian equation for the orbit path:

$$\left(\frac{x - \sqrt{a^2 - b^2}}{a}\right)^2 + \left(\frac{y}{b}\right)^2 = 1 \tag{6}$$

Now we convert this to polar coordinates. We replace x with $r\cos\theta$ and y with $r\sin\theta$, and after simplification, we arrive at the quadratic:

$$(a^2\sin^2(\theta) + b^2\cos^2(\theta))r^2 - (2ab^2\epsilon\cos(\theta))r - b^4 = 0 \tag{7}$$

Solving this quadratic using the quadratic formula, and taking only positive roots of r as valid answers, we arrive at the final polar form:

$$r = \frac{a(1 - \epsilon^2)}{1 - \epsilon\cos\theta} \tag{8}$$

To plot 3D orbits, we have to transform the 2D x and y coordinates to new x, y, and z coordinates in 3D space. We do this using matrices, assuming we rotate clockwise about the y-axis. It is well known that a rotation of angle θ clockwise about the y-axis is represented by the matrix:

$$R_\theta = \begin{bmatrix} \cos(\theta) & 0 & -\sin(\theta) \\ 0 & 1 & 0 \\ \sin(\theta) & 0 & \cos(\theta) \end{bmatrix} \tag{9}$$

Therefore, the 2D coordinates after transformation become:

$$\begin{bmatrix} x' \\ y' \\ z' \end{bmatrix} = R_\theta \begin{bmatrix} x \\ y \\ 0 \end{bmatrix} = \begin{bmatrix} \cos(\theta) & 0 & -\sin(\theta) \\ 0 & 1 & 0 \\ \sin(\theta) & 0 & \cos(\theta) \end{bmatrix} \begin{bmatrix} x \\ y \\ 0 \end{bmatrix} = \begin{bmatrix} x\cos(\theta) \\ y \\ x\sin(\theta) \end{bmatrix} \tag{10}$$

4 Calculating Polar Angle from Time Elapsed

Kepler's 2nd Law tells us that:

$$\frac{1}{2}r^2\frac{\mathrm{d}\theta}{\mathrm{d}t} = \frac{1}{2}\sqrt{G(M+m)(1-\epsilon^2)a} \tag{11}$$

This leads to:

$$t = P(1-\epsilon^2)^{\frac{3}{2}}\frac{1}{2\pi}\int_0^\theta \frac{1}{(1-\epsilon\cos\theta)^2}\,d\theta \tag{12}$$

For small angles, the integrand in Eq.9 can be approximated with a binomial expansion to the second order term (noting that $|\epsilon\cos\theta| < 1$ for elliptical orbits) to give:

$$t \approx P(1-\epsilon^2)^{\frac{3}{2}}\frac{1}{2\pi}\int_0^\theta 1 + 2\epsilon\cos\theta + 3\epsilon^2\cos^2\theta\,d\theta \tag{13}$$

$$t \approx P(1-\epsilon^2)^{\frac{3}{2}}\frac{1}{2\pi}(\theta + \frac{3}{2}\epsilon^2\theta + 2\epsilon\sin\theta + \frac{3}{4}\epsilon^2\sin 2\theta) \tag{14}$$

This approximates the time elapsed well for small eccentricities, but for larger eccentricities it loses a lot of accuracy (as is common with all binomial expansion approximations). To find the polar angle from the time elapsed, iterative methods or the Newton-Raphson method can be used, which may converge on a solution for θ faster than interpolating from a graph using numpy.

The second method is to use Simpson's method to numerically calculate the value of the integral in Eq.9. This method takes $O(n)$ time complexity to find a solution, as if the required end θ value is increased, the time taken to calculate the extra x and y values up to that θ value increases proportionally. Furthermore, the time taken for numpy.interp() to perform linear interpolation on the data also varies proportionally with the length of the data. Fig.1 is a graph of angular displacement vs time for two eccentricities, calculated by using Simpson's rule with an increment of $h = 1/1000$.

We can see that our binomial expansion predicts the form of the curve for $\epsilon = 0.25$ in Figure 2, as it appears to be a sine curve overlaid on a straight line, which is exactly the form of our binomial approximation in Eq.11 to the order of ϵ (ϵ^2 is very small in this case, so the associated terms do not make a significant difference to the form of the curve).

5 Plotting Orbits of Planets Relative to Other Planets

Let the position vector of the planet in the Sun's reference frame be $\vec{r}$. The planet from its reference frame is stationary, and so it follows that the position vector of the Sun from the planet's reference frame is $-\vec{r}$. This vector can then be added to the position vectors of all other planets from the Sun's reference frame to plot the desired paths.

For example, relative to Saturn, the other planets follow the paths in Figure 3.

These orbital paths resemble the patterns created by spirographs, and it is possible to analyse these patterns further to predict the paths of other planets.

The parametric equation of these spirographs for circular orbits is clearly:

$$x = -r_1\cos(\omega_1 t) + r_2\cos(\omega_2 t) \tag{15}$$

$$y = -r_1\sin(\omega_1 t) + r_2\sin(\omega_2 t) \tag{16}$$

where r_1 and ω_1 are the radius and angular velocities of the star's orbit, and r_2 and ω_2 are the radius and angular velocities of the planet's orbit. Without loss of generality, we assume throughout that $\omega_1 < \omega_2$.

In Figure 3, we can see several loops or 'cusps' that are formed in the resulting pattern. These clearly occur when the distance from the curve to the origin is a minimum. From the parametric equation above:

Figure 2: A graph of orbit polar angle vs time

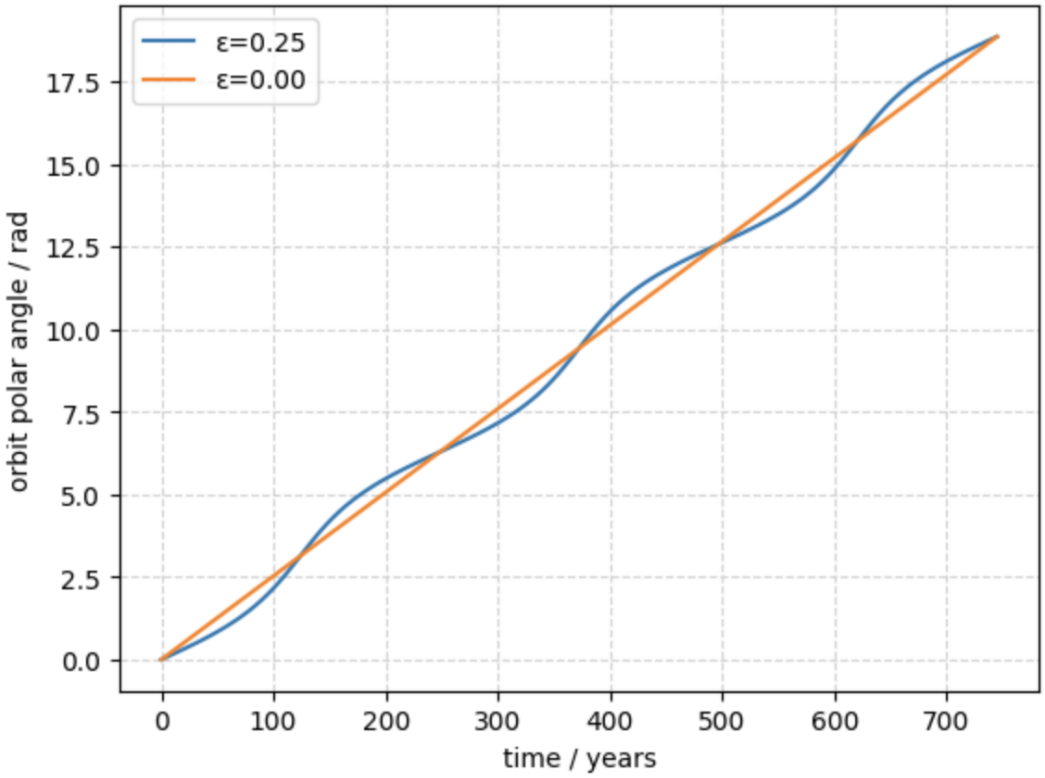

Reference Planet (Planet 1)	Other Planet (Planet 2)	$\frac{10(\omega_2-\omega_1)}{\omega_1}+1$	Observed Cusp Centres
b	f	8.79	8
b	d	6.46	6
d	f	6.14	6
d	g	9.07	9
g	e	27.9	27

Table 1: Shows the strong correlation between our predicted result for the number of cusps and the actual number of observed cusps formed in 10 star orbits of the reference planet

$$\begin{aligned} d^2 &= x^2 + y^2 \\ &= (-r_1\cos(\omega_1 t) + r_2\cos(\omega_2 t))^2 + (-r_1\sin(\omega_1 t) + r_2\sin(\omega_2 t))^2 \\ &= r_1^2 + r_2^2 - 2r_1r_2\cos(\omega_2 t)\cos(\omega_1 t) - 2r_1r_2\sin(\omega_2 t)\sin(\omega_1 t) \\ &= r_1^2 + r_2^2 - 2r_1r_2\cos((\omega_2-\omega_1)t) \end{aligned} \tag{17}$$

Equation 17 reveals a number of important properties of these parametric curves. Firstly, $-1 \leq \cos((\omega_2-\omega_1)t) \leq 1$, so each point of the curve is always a distance of between $r_1 - r_2$ and $r_1 + r_2$ away from the origin. Secondly, a centre of a cusp is when the distance to the origin is a minimum, or when $\cos((\omega_2-\omega_1)t_{cusp}) = -1$ and $t_{cusp} = \frac{2\pi n}{\omega_2-\omega_1}$ and so in one full orbit of planet 1, t varies from 0 to $\frac{2\pi}{\omega_1}$, so there are $\lfloor\frac{\omega_2-\omega_1}{\omega_1}\rfloor + 1$ centres of cusps formed.

We can test this result by using the exoplanets from the Kepler-11 system. Each of the spirographs referenced in Table 1 are included in the appendix. Note that the spirographs are for 10 star orbits for the reference planet.

Not only is this strong evidence for the hypothesis, but the fractional part of the predicted value also gives us an indication of how far away in time the next cusp will be.

Let us study these cusps further. If the cusp forms a 'loop', then for some x, the x value of the curve at $t = t_{cusp} - x$ must be the same as the x value of the curve at $t = t_{cusp} + x$. Thus:

$$\begin{aligned} -r_1 \cos(\omega_1(t_{cusp} - x)) + r_2 \cos(\omega_2(t_{cusp} - x)) &= -r_1 \cos(\omega_1(t_{cusp} + x)) + r_2 \cos(\omega_2(t_{cusp} + x)) \\ 2r_1 \sin(\omega_1 t_{cusp}) \sin(\omega_1 x) &= 2r_2 \sin(\omega_2 t_{cusp}) \sin(\omega_2 x) \end{aligned} \tag{18}$$

Note that from Equation 18, $t_{cusp} = \frac{2\pi n}{\omega_2 - \omega_1}$. This means that $\omega_2 t_{cusp} - \omega_1 t_{cusp} = 2\pi n$, so Equation 18 simplifies to:

$$r_1 \sin(\omega_1 x) = r_2 \sin(\omega_2 x) \tag{19}$$

So cusps form loops only if there is a solution for x in Equation 19. If we differentiate both sides, we get:

$$r_1 \omega_1 \cos(\omega_1 x) = r_2 \omega_2 \cos(\omega_2 x) \tag{20}$$

Clearly, $\omega_1 < \omega_2$, as otherwise cusps would not be formed. First, assume that $r_1\omega_1 > r_2\omega_2$. At $x = 0$, the gradient of the left hand side is greater than the gradient of the right hand side, and because $\omega_1 < \omega_2$, $\cos(\omega_1 x > \omega_2 x)$ for all $0 \leq x < \frac{2\pi}{\omega_2}$ according to Equation 20. Therefore, there are solutions to Equation 15 in the interval $0 < x < \frac{2\pi}{\omega_2}$ if and only if $r_1\omega_1 < r_2\omega_2$. Therefore, cusps are only formed if and only if $r_1\omega_1 < r_2\omega_2$. In other words, the tangential velocity of the planet that is stationary in the reference frame must be less than the tangential velocity of the other planet for 'loops' to form.

An approximate value for x can also be found by using the small angle approximation $\sin(x) \approx x - x^3/6$. This yields:

$$r_1\omega_1 x - \frac{r_1\omega_1^3 x^3}{6} \approx r_2\omega_2 x - \frac{r_2\omega_2^3 x^3}{6}$$

$$x \approx \pm\sqrt{\frac{6(r_2\omega_2 - r_1\omega_1)}{r_2\omega_2^3 - r_1\omega_1^3}} \tag{21}$$

This value of x can then be plugged into Equation 17 to find the length of a cusp. This length is:

$$l = \sqrt{r_1^2 + r_2^2 - 2r_1 r_2 \cos((\omega_2 - \omega_1)(t_{cusp} - x))} - \sqrt{r_1^2 + r_2^2 - 2r_1 r_2 \cos((\omega_2 - \omega_1) t_{cusp})}$$

$$l = \sqrt{r_1^2 + r_2^2 - 2r_1 r_2 \cos((\omega_2 - \omega_1)(t_{cusp} - x))} - (r_1 - r_2) \tag{22}$$

This approximation performs best at small values of x, or when the cusps formed are small. It loses a lot of accuracy on larger cusps. However, more accuracy could be achieved on this case by using numerical methods to calculate the value of x using Equation 19.

It is worth noting again that all of this mathematical analysis of spirographs applies only for circular orbits. For slightly elliptical orbits such as the ones in the solar system, cusps will vary in size, will not be positioned in regular intervals, and the bounds on the distance of the path away from the origin will vary with time, as can be seen in Figure 3.

Figure 3: Orbits of outer solar system relative to Saturn (6 solar orbits)

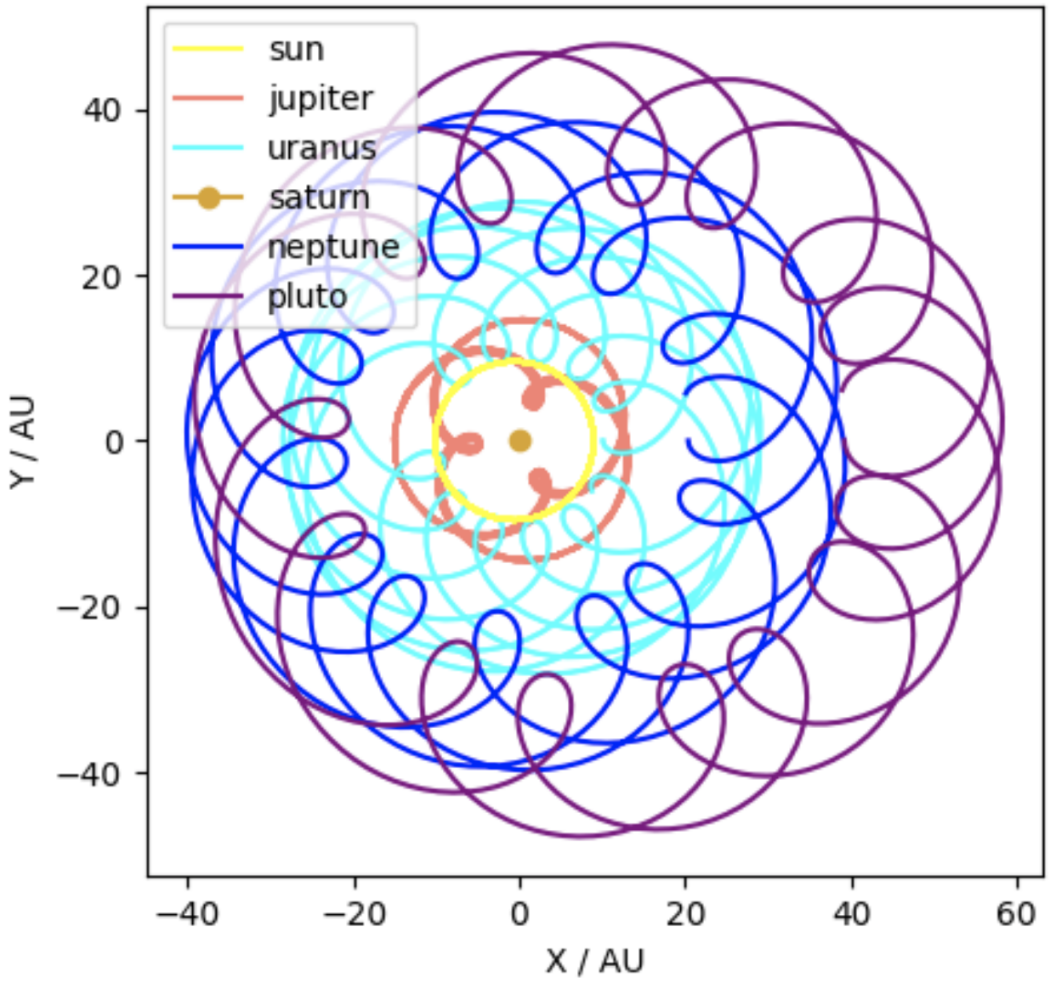

Figure 4: Orbit of planet f relative to planet b in Kepler-11 System (10 star orbits)

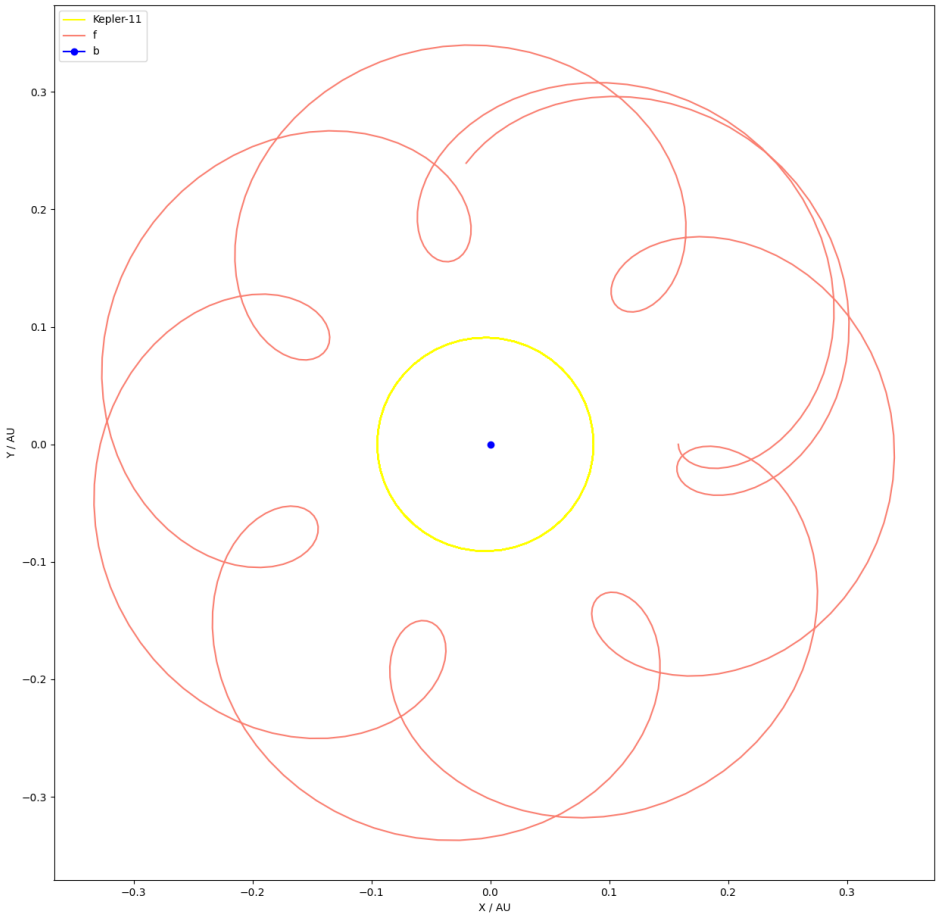

Figure 5: Orbit of planet d relative to planet b in Kepler-11 System (10 star orbits)

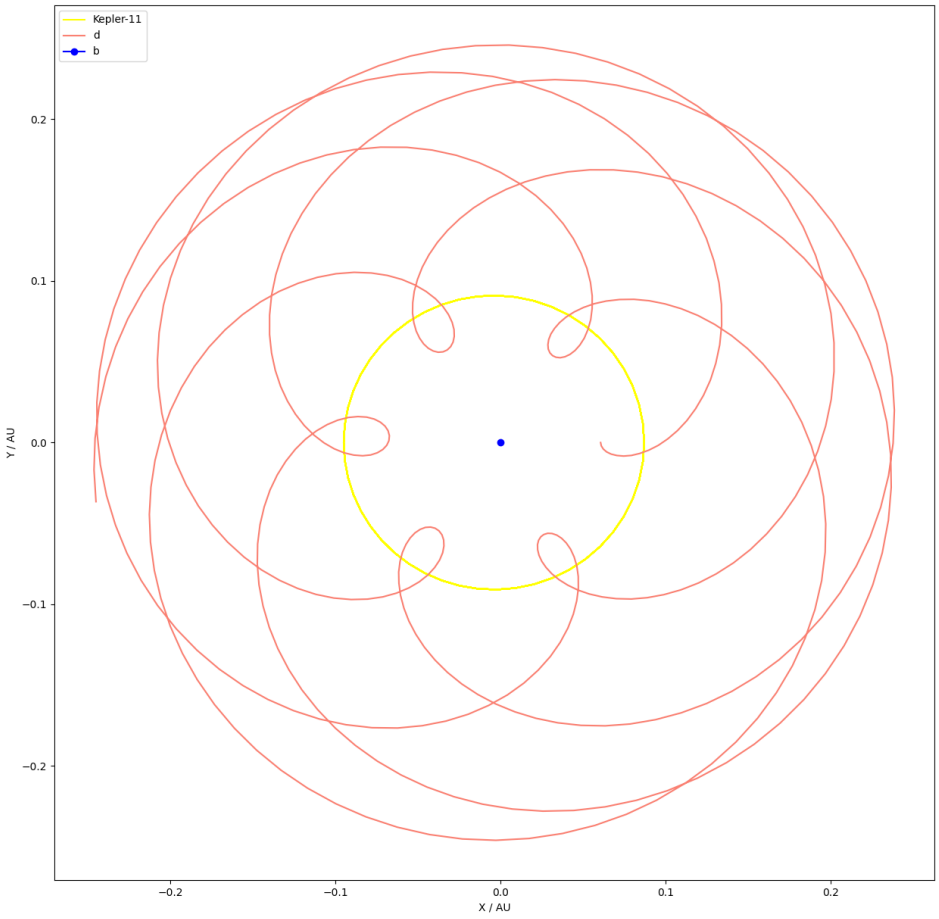

Figure 6: Orbit of planet f relative to planet d in Kepler-11 System (10 star orbits)

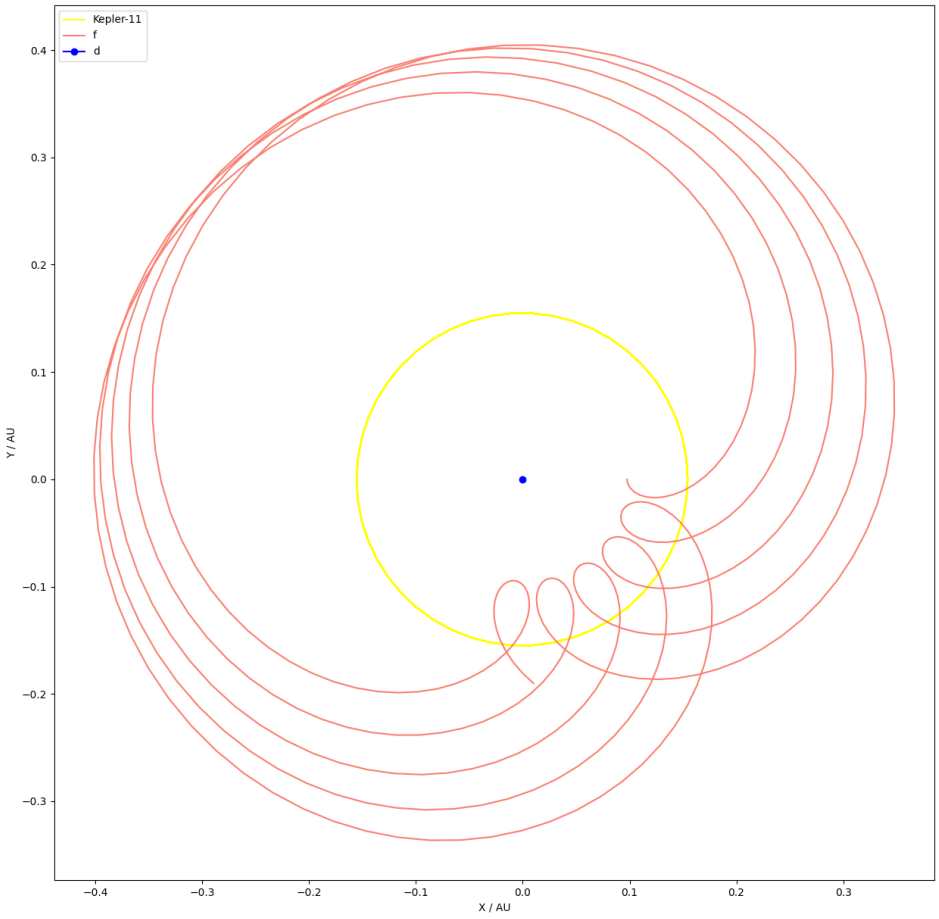

Figure 7: Orbit of planet g relative to planet d in Kepler-11 System (10 star orbits)

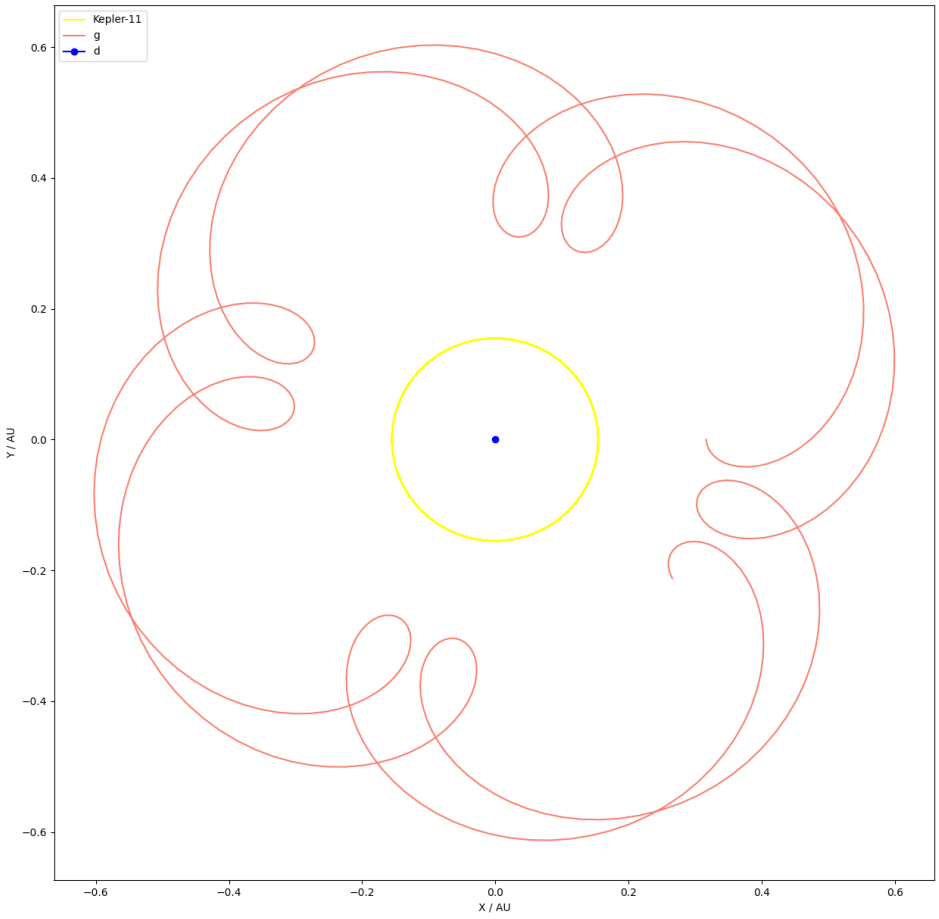

Figure 8: Orbit of planet e relative to planet g in Kepler-11 System (10 star orbits)